

# A Protonated Water Cluster as a Transient Proton-Loading Site in Cytochrome *c* Oxidase

Shreyas Supekar, Ana P. Gamiz-Hernandez, and Ville R. I. Kaila\*

**Abstract:** Cytochrome *c* oxidase (CcO) is a redox-driven proton pump that powers aerobic respiratory chains. We show here by multi-scale molecular simulations that a protonated water cluster near the active site is likely to serve as the transient proton-loading site (PLS) that stores a proton during the pumping process. The  $pK_a$  of this water cluster is sensitive to the redox states of the enzyme, showing distinct similarities to other energy converting proton pumps.

Cytochrome *c* oxidase (CcO) is the terminal electron acceptor enzyme that drives aerobic respiratory chains in mitochondria and bacteria.<sup>[1]</sup> CcO receives electrons from the soluble cytochrome *c*, and transfers them to molecular oxygen, which is reduced to water in the binuclear heme  $a_3$ /Cu<sub>B</sub> active site (BNC, Figure 1). The free energy released in the process is coupled to proton pumping across the biological membrane. Experimental and computational studies<sup>[2]</sup> have given detailed insights into the structure and function of the

proton pump, but the exact molecular mechanism that CcO employs for proton pumping, nevertheless, still remains unsolved.<sup>[1b,c]</sup>

The electron transfer (eT) in CcO through Cu<sub>A</sub>, heme *a*, to the BNC, thermodynamically drives two proton-transfer (pT) processes; the chemical protons are transferred to the BNC to complete the O<sub>2</sub> chemistry, whereas the pumped protons are transferred against the membrane potential to the positively charged (P)-side of the membrane (Figure 1). The proton-conducting D- and K-channels are employed for uptake of chemical protons, whereas all pumped protons originate from the D-channel.<sup>[1b,c]</sup> Time-resolved experiments<sup>[2b,c]</sup> suggest that the pumped protons are transiently stored at an unknown proton-loading site (PLS), before they are ejected across the membrane. The PLS thus plays an important role in transducing the free energy released from the reduction chemistry at the BNC into pumping protons across the membrane. Moreover, the PLS is most likely involved in preventing the protons from leaking backwards in the pumping step towards their thermodynamically favorable direction.<sup>[1b,2h]</sup>

Belevich et al.<sup>[2b,c]</sup> suggested that the PLS is protonated in 150 μs by Glu-242, located at the end of the proton-conducting D-channel (Figure 1, but cf. Ref. [3]), while reduction and protonation of the BNC led to release of the proton from the PLS to the P-side of the membrane in about 2.6 ms. Experimentally, it is nevertheless challenging to rule out if the BNC reduction takes place concertedly with loading of the PLS.<sup>[1c]</sup> It was suggested<sup>[2c]</sup> that the PLS could reside above heme  $a_3$ , for example, at the D- or A-propionate sites of heme  $a_3$ . Svensson-Ek et al.<sup>[4]</sup> observed structural changes around the D-propionate of heme  $a_3$  (D-prp) when Glu-242 was mutated into a glutamine, and Sharpe et al.<sup>[5]</sup> found that the Mg<sup>2+</sup> center, located about 6 Å from the D-prp, underwent electronic transitions during the pumping process. No direct infrared signals have so far been linked to the protonation of the PLS,<sup>[2e,6]</sup> but Iwaki and Rich<sup>[2e]</sup> found that reduction of the heme *a* leads to spectral changes that might reflect vibrational shifts in guanidinium groups of Arg-438 (Figure 1), which forms an ion-pair with the D-prp. Electrostatic calculations<sup>[2k,7]</sup> further suggested that reduction of heme *a* might lead to an increase in the  $pK_a$  of several sites above heme  $a_3$ , but the exact location of the PLS, nevertheless, still remains unclear.

We show here using multi-scale molecular simulations of CcO that a protonated water cluster above the active site in CcO can transiently store a proton as a Zundel or Eigen-ion, and that its  $pK_a$  is sensitive to the redox state of the enzyme. Our results are based on density functional theory (DFT) models and hybrid quantum mechanics/molecular mechanics

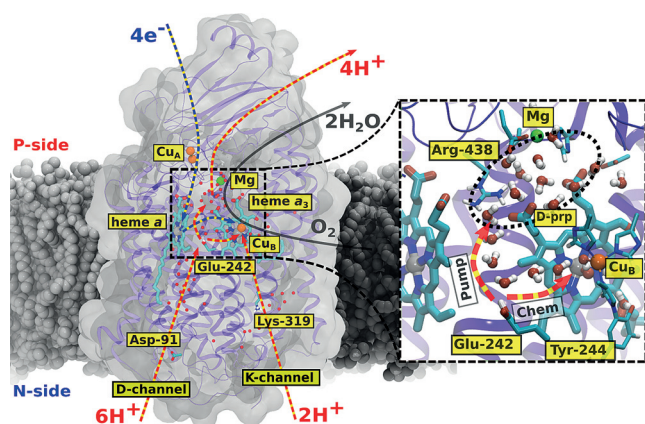


**Figure 1.** The structure and function of cytochrome *c* oxidase (CcO). Reduction of O<sub>2</sub> to water drives electron transfer (blue arrows) from cytochrome *c* (not shown) via Cu<sub>A</sub> and heme *a* to the heme  $a_3$ /Cu<sub>B</sub> center that leads to uptake of protons (red arrows) from the negatively charged (N) side of the membrane using the D- and K-channels. Glu-242, at the end of the D-channel, transfers protons both to the BNC and to the proton-loading site (PLS) above heme  $a_3$ , from which the protons are released to the positively (P)-side of the membrane. Inset: The active site, and the nonpolar cavity above Glu-242. The PLS region is indicated with a dotted circle.

[\*] S. Supekar, Dr. A. P. Gamiz-Hernandez, Prof. Dr. V. R. I. Kaila  
Department Chemie, Technische Universität München (TUM)  
Lichtenbergstraße 4, 85747 Garching (Germany)  
E-mail: ville.kaila@ch.tum.de

Supporting information for this article can be found under:  
<http://dx.doi.org/10.1002/anie.201603606>.

(QM(DFT)/MM MD) simulations, which provide an accurate energetic description of bond-formation and bond-breakage chemistries (Table S3), and allow us to probe the dynamics of the PLS.

The X-ray structures of CcO lack water molecules in the nonpolar region above Glu-242 that catalyze the pT process along the chemistry and pumping pathways.<sup>[1b,2a,8]</sup> We therefore performed classical MD simulations of CcO with four to six water molecules inserted in the nonpolar cavity as suggested from earlier calculations.<sup>[2g,h,9]</sup> Based on the MD structures, we addressed the energetics and structure of likely protonation sites above heme  $a_3$  with large-scale quantum chemical DFT and QM/MM MD simulations in states that mimic the pumping cycle, prior and after reduction of heme  $a$  ( $a^{\text{ox}}/a^{\text{red}}$ ) with the BNC in the experimentally observed  $P_M$  (“oxidized”),  $P_R$  (“reduced”), or F (“reduced + protonated”) states (see the Supporting Information). Our models comprise the active site together with nearby protein residues and water molecules, and range in size from 150–340 atoms, and are thus likely to have reached convergence with respect to the size of the QM region.<sup>[10]</sup> Upon QM optimization, we find that the proton, initially placed on the D-prp of heme  $a_3$ , moves in the structure optimization to the water cluster above this site, forming a protonated Zundel-like ( $\text{H}_3\text{O}_2^+$ ) water cluster, bridging the D-prp and Glu-198/Asp-369 of the  $\text{Mg}^{2+}$  center (Figure 2A). We obtain a state that mimics the protonation of the PLS, and is about 8 kcal mol<sup>−1</sup> higher in energy relative to the initial state with Glu-242 protonated (Table S1). This slightly endergonic process is consistent with previous thermodynamic analysis of the pumping-process.<sup>[11]</sup> We find that the protonated water cluster is also stable in several alternative states (see Figure S1 in the Supporting Information), and resembles either Zundel ( $\text{H}_5\text{O}_2^+$ ) or Eigen ( $\text{H}_3\text{O}^+$ ) structures,<sup>[12]</sup> possibly reflecting the dynamical nature of the proton. We also attempted protonation of the A-propionate of heme  $a_3$  but this resulted in optimized structures that were much higher in energy or led to relaxation of the proton back to the water cluster (Figure S2).

From the DFT models we find that protonation and reduction of the BNC, yielding the F state, results in the decrease of the proton affinity of the water cluster by about 9 kcal mol<sup>−1</sup>, while protonation of the PLS increases the electron affinity of the BNC by 0.3 eV (Table S1). These electronic energies are consistent with previous results,<sup>[1b,2b,c,11a,13]</sup> suggesting that the protonation of the PLS, leads to reduction of the BNC, while protonation and reduction of the BNC is coupled to ejection of the proton to the P-side of the membrane.

To probe whether the protonated water cluster remains dynamically stable also at  $T = 310$  K, we performed QM/MM MD simulations on the protonated and deprotonated forms of the PLS. Snapshots of the QM/MM trajectories are shown in Figure 2B. We find that the protonated water cluster indeed remains stable on picosecond timescales, and is delocalized on the two water molecules between the D-prp and Asp-364/Glu-198. The water cluster is also stable without the proton (Figure S3), and also after 10 ns MD relaxation (Figure S14). In the  $a^{\text{red}}/P_M$  state the Zundel ion partially dissociates to Glu-198 (Figure 2C), which may reflect that the PLS may re-

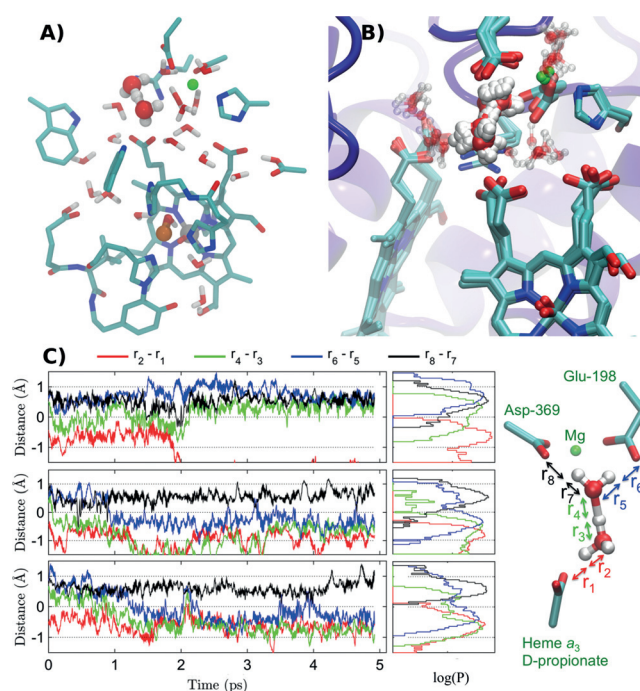


**Figure 2.** Structure and dynamics of the protonated water cluster above the D-propionate of heme  $a_3$ . A) Optimized protonated water cluster in the  $P_M$  state from a DFT model with 340 atoms. B) Snapshots from QM/MM dynamics of the protonated water cluster from a 5 ps trajectory with about 130 QM atoms and about 88 700 MM atoms. C) QM/MM dynamics and probability distributions of the central oxygen-hydrogen distance differences, shown in inset to the right. A value near 0 Å, indicates a proton shared between two oxygens, while values  $> +1.0$  /  $< -1.0$  Å indicate regular hydrogen bonds. The three panels show the dynamics in the  $a^{\text{ox}}/P_M$  (top),  $a^{\text{red}}/P_M$  (middle),  $a^{\text{ox}}/F$  (bottom) states.

distribute among several sites, having a rather shallow energy surface, as suggested by recent continuum electrostatic calculations.<sup>[7c]</sup> We observe that reduction of heme  $a$  increases the proton affinity of the PLS by 4–10 kcal mol<sup>−1</sup> (Table S1), as obtained from QM/MM single-point energy calculations or classical electrostatic calculations on the QM/MM trajectories (Figure S4). By calculating the vibrational spectrum from the QM/MM MD trajectories, we find that the protonation of water cluster leads to disappearance of vibrational peaks at 3600–3800 cm<sup>−1</sup> (Figure S5), which have been assigned to weakly hydrogen-bonded dangling water molecules in FTIR studies.<sup>[6a,b]</sup> Interestingly, similar signals have also been associated with protonated water clusters in bacteriorhodopsin.<sup>[6b]</sup> Our QM models further suggest that hydronium has vibrational modes at 1770–2670 cm<sup>−1</sup> (Table S2, Figure S5B), and shifts linked to the guanidinium group of Arg-438 upon protonation of PLS from that may relate to findings by Iwaki and Rich.<sup>[2e]</sup> Vibrational frequencies can, however, be subjected to large anharmonic effects for species such as the  $\text{H}_3\text{O}^+$ .<sup>[14]</sup>

To probe how the cluster is protonated by Glu-242, we also performed unrestrained QM/MM MD simulations with a hydronium next to a neutral Glu-242, a transient species mimicking a concerted proton transfer from the D-channel, as suggested by recent semi-empirical QM/MM studies.<sup>[15a]</sup> In



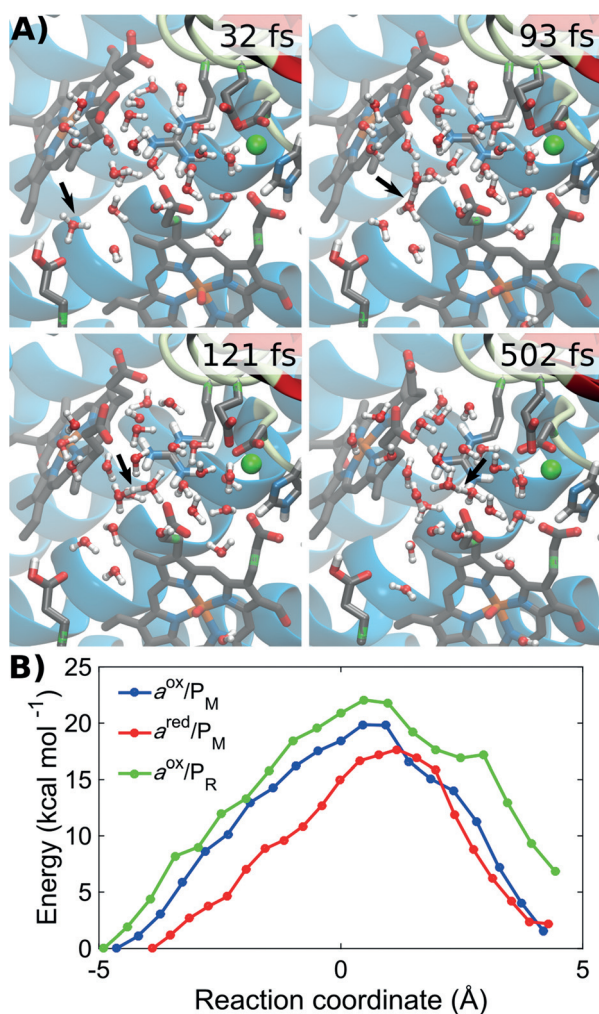


**Figure 3.** QM/MM simulations of the pT from Glu-242 to the PLS. A) In the  $a^{\text{red}}/P_M$  (red/ox) state, Glu-242 protonates the water cluster above heme *a*<sub>3</sub> in 0.5 ps along the water chain that forms in classical MD simulations. The pT takes place by a semi-concerted Grotthuss-type transfer mechanism (S1). The QM/MM MD simulation was initiated by adding a hydronium near a neutral Glu-242, mimicking a concerted proton uptake from the D-channel. B) pT reaction profiles at B3LYP-D3/def2-TZVP level for the loading of PLS from a neutral Glu-242 (without added hydronium) in  $a^{\text{red}}/P_M$  (red; red/ox),  $a^{\text{ox}}/P_M$  (blue; ox/ox),  $a^{\text{ox}}/P_R$  (green; ox/red) states. Reaction profiles at B3LYP-D3/def2-SVP level are shown in Figure S7.

these simulations, we observed spontaneous pT using a Grotthuss-type hopping mechanism, shown in Figure 3A, with intermediate Zundel ( $\text{H}_5\text{O}_2^+$ ) and hydronium ( $\text{H}_3\text{O}^+$ )-type structures. This pT process takes place semi-concertedly, typical for pT in short water wires,<sup>[17]</sup> and leads to formation of the protonated water cluster above the D-prp in 0.5 ps (Figure S6). To further understand the dependence of redox states on this pT, we performed QM/MM reaction path optimizations of the pT from a neutral Glu-242 to the PLS. We obtain a pT barrier of 12–18 kcal mol<sup>-1</sup> in the  $a^{\text{red}}/P_M$  state (Figure 3B, Figure S7), which is consistent with free energy profiles obtained from previous EVB calculations.<sup>[21j]</sup> Our calculations further suggest that in states with heme *a* oxidized ( $a^{\text{ox}}/P_M$  and  $a^{\text{ox}}/P_R$ ) the barrier increases to 20–

22 kcal mol<sup>-1</sup>, suggesting that the redox state of heme *a* electrostatically controls the pT barrier, also in the case that pT takes place from a neutral Glu-242,<sup>cf.[13]</sup> and may thus provide a gating element preventing proton backflow. Reaction scans can, however, be sensitive to local changes in the protein environment,<sup>[16]</sup> for example, the Trp-126/D-prp hydrogen-bond, which is broken in our simulations (Figure S13), resembling configurations described by Goyal et al.<sup>[15b]</sup> Our solvation free-energy calculations, nevertheless, also support that the electron on heme *a* lowers the pT barrier by up to 4 kcal mol<sup>-1</sup> (Figure S11). Moreover, rotation of the anionic Glu-242 towards the D-channel, and its rapid re-protonation might further contribute in preventing the proton from leaking back to Glu-242.<sup>[2h,j,m]</sup> (Figure S9). The barrier for the PLS loading in the  $a^{\text{red}}/P_M$  state is in good agreement with the experimental barrier of about 13 kcal mol<sup>-1</sup>.<sup>[2b,c]</sup> Based on our benchmarking calculations (Tables S3 and S4), the employed DFT-method captures the proton affinity differences between carboxylates and water clusters with an accuracy of about 2 kcal mol<sup>-1</sup> relative to correlated calculations. Moreover, entropic effects might further reduce the barriers by about 3 kcal mol<sup>-1</sup> based on model calculations of pT in water wires.<sup>[17b]</sup> Tunneling effects based on measured H/D kinetic isotopic effects in CcO are expected to have a small contribution on the barriers.<sup>[18]</sup>

We find that in all available high-resolution X-ray structures of CcO, the water molecules involved in forming the protonated water cluster near the propionic groups of heme *a*<sub>3</sub> are structurally conserved (Figure S8). Moreover, the water structure involved in forming the protonated cluster remains stable during several hundred nanosecond MD simulations (Figure S10). If the water molecules involved in forming the putative PLS are functionally important, it would also imply that a “dry” PLS region might lead to a compromised proton-pumping activity, which can be observed under certain experimental conditions, such as in the resting oxidized (O) state.<sup>[1b,c]</sup> Reduction and re-oxidation can be used for re-activation of the O state into a pumping O<sub>H</sub> state, which is also linked to synthesis of new water molecules at the BNC, and could further “re-wet” the PLS. Previous MD simulations<sup>[19]</sup> indeed suggest that water molecules leave the nonpolar cavity above Glu-242 via opening of the D-prp/Arg-438 ion pair. QM/MM free-energy calculations can provide important generalization of the coupling between the hydration dynamics and the pumping energetics in CcO, but such simulations are currently outside the scope of our present work.

The identified water cluster has an interesting resemblance to the proton-release group (PRG) of the light-driven proton pump, bacteriorhodopsin (bR), which serves a similar functional role as PLS. Experimental studies<sup>[6b]</sup> suggest that the PRG in bR may comprise a protonated water cluster bridging between Glu-194/Glu-204 and Arg-82, resembling our suggested PLS site in CcO. However, recent semi-empirical calculations on bR<sup>[20]</sup> suggest that the nearby protein residues prefer the proton to the water cluster.

In summary, we have shown here that a structurally conserved water cluster may function as a transient proton-loading site (PLS) in CcO. Our simulations suggest that

protonation of this water cluster is sensitive to the redox-state of the enzyme, and takes place by water-mediated Grotthuss-type transfer mechanism from Glu-242. The water cluster remained stable in both large-scale quantum chemical calculations and QM/MM dynamics simulations on picosecond timescales. Consistent with experiments, we also found that protonation of this cluster increases the redox-potential of the active site, while reduction and protonation of the latter was coupled to the decrease of its  $pK_a$  that is likely to couple to the release of the proton to the P-side of the membrane. Our multi-scale simulations suggest that water molecules in CcO provide important coupling elements with distinct similarities to other energy converting proton pumps such as bacteriorhodopsin<sup>[6b]</sup> and the respiratory complex I.<sup>[21]</sup>

## Methods

MD models were built based on the X-ray structure bovine CcO (PDB ID: 1V54),<sup>[2a]</sup> with subunits I-II embedded in a POPC membrane and solvated with TIP3P water, and 100 mM NaCl. The system was relaxed for 10 ns, at  $T = 310$  K with a 1 fs integration time step with NAMD<sup>[22]</sup> using the CHARMM27 force field<sup>[23]</sup> and in-house parameters.<sup>[24]</sup> QM and QM/MM models were based on relaxed MD structures. QM/MM MD were carried out for 5 ps and reaction pathway optimizations were performed using a linear combination of the pT-coordinates (see the Supporting Information). The QM region comprised about 130 atoms described at BP86-D3/def2-SVP or B3LYP-D3/def2-SVP levels<sup>[26]</sup> and the remaining system treated at the MM level. The QM cluster models with about 340 atoms were optimized at BP86-D3/def2-SVP/def2-TZVP (Fe, Cu) level<sup>[27]</sup> and the COSMO model<sup>[28]</sup> with  $\epsilon = 4$ . Single point calculations were carried out at the B3LYP-D3/def2-SVP/def2-TZVP (Fe, Cu) level.<sup>[26a,c]</sup> TURBOMOLE v6.5-6.6<sup>[29]</sup> was employed for the QM calculations, CHARMM/Q-Chem for QM/MM,<sup>[25]</sup> and VMD<sup>[30]</sup> for visualization. Details of the computational methods can be found in the Supporting Information.

## Acknowledgements

We acknowledge Prof. Dr. Mårten Wikström for insightful discussions. The German Research Foundation (DFG), the Jane and Aatos Erkko foundations, and the German-Exchange Service (DAAD) financially supported this research. We acknowledge Supermuc (grant: pr84gu) at the Leibniz-Rechenzentrum, and the Finnish IT Center for Science for providing computational resources.

**Keywords:** bioenergetics · electron transfer · enzymes · molecular dynamics · proton transfer

**How to cite:** *Angew. Chem. Int. Ed.* **2016**, *55*, 11940–11944  
*Angew. Chem.* **2016**, *128*, 12119–12123

- [1] a) M. K. F. Wikström, *Nature* **1977**, *266*, 271–273; b) V. R. I. Kaila, M. I. Verkhovsky, M. Wikström, *Chem. Rev.* **2010**, *110*,

- 7062–7081; c) M. Wikström, V. Sharma, V. R. I. Kaila, J. P. Hosler, G. Hummer, *Chem. Rev.* **2015**, *115*, 2196–2221.  
[2] a) T. Tsukihara, et al., *Proc. Natl. Acad. Sci. USA* **2003**, *100*, 15304–15309; b) I. Belevich, M. I. Verkhovsky, M. Wikström, *Nature* **2006**, *440*, 829–832; c) I. Belevich, D. A. Bloch, N. Belevich, M. Wikström, M. I. Verkhovsky, *Proc. Natl. Acad. Sci. USA* **2007**, *104*, 2685–2690; d) K. Faxén, G. Gilderson, P. Ådelroth, P. Brzezinski, *Nature* **2005**, *437*, 286–289; e) M. Iwaki, P. R. Rich, *J. Am. Chem. Soc.* **2007**, *129*, 2923–2929; f) G. Bränden, A. S. Pawate, R. B. Gennis, P. Brzezinski, *Proc. Natl. Acad. Sci. USA* **2006**, *103*, 317–322; g) M. Wikström, M. I. Verkhovsky, G. Hummer, *Biochim. Biophys. Acta Bioenerg.* **2003**, *1604*, 61–65; h) V. R. I. Kaila, M. I. Verkhovsky, G. Hummer, M. Wikström, *Proc. Natl. Acad. Sci. USA* **2008**, *105*, 6255–6259; i) A. V. Pislakov, P. K. Sharma, Z. T. Chu, M. Haranczyk, A. Warshel, *Proc. Natl. Acad. Sci. USA* **2008**, *105*, 7726–7731; j) T. Yamashita, G. A. Voth, *J. Am. Chem. Soc.* **2012**, *134*, 1147–1152; k) E. Fadda, C. H. Yu, R. Pomes, *Biochim. Biophys. Acta Bioenerg.* **2008**, *1777*, 277–284; l) S. A. Siletsky, A. S. Pawate, K. Weiss, R. B. Gennis, A. A. Konstantinov, *J. Biol. Chem.* **2004**, *279*, 52558–52565; m) A. L. Woelke, G. Galstyan, A. Galstyan, T. Meyer, J. Heberle, E.-W. Knapp, *J. Phys. Chem. B* **2013**, *117*, 12432–12441.  
[3] H. Lepp, E. Svahn, K. Faxén, P. Brzezinski, *Biochemistry* **2008**, *47*, 4929–4935.  
[4] M. Svensson-Ek, J. Abramson, G. Larsson, S. Törnroth, P. Brzezinski, S. Iwata, *J. Mol. Biol.* **2002**, *321*, 329–339.  
[5] M. A. Sharpe, M. D. Krzyaniak, S. Xu, J. McCracken, S. Ferguson-Miller, *Biochemistry* **2009**, *48*, 328–335.  
[6] a) A. Marechal, P. R. Rich, *Proc. Natl. Acad. Sci. USA* **2011**, *108*, 8634–8638; b) F. Garczarek, K. Gerwert, *Nature* **2006**, *439*, 109–112; c) R. M. Nyquist, D. Heitbrink, C. Bolwien, R. B. Gennis, J. Heberle, *Proc. Natl. Acad. Sci. USA* **2003**, *100*, 8715–8720.  
[7] a) V. R. I. Kaila, V. Sharma, M. Wikström, *Biochim. Biophys. Acta Bioenerg.* **2011**, *1807*, 80–84; b) D. M. Popovic, A. A. Stuchebrukhov, *J. Am. Chem. Soc.* **2004**, *126*, 1858–1871; c) J. Lu, M. R. Gunner, *Proc. Natl. Acad. Sci. USA* **2014**, *111*, 12414–12419.  
[8] a) S. Iwata, C. Ostermeier, B. Ludwig, H. Michel, *Nature* **1995**, *376*, 660–669; b) J. Liu, L. Qin, S. Ferguson-Miller, *Proc. Natl. Acad. Sci. USA* **2011**, *108*, 1284–1289; c) V. Sharma, G. Enkavi, I. Vattulainen, T. Rog, M. Wikström, *Proc. Natl. Acad. Sci. USA* **2015**, *112*, 2040–2045.  
[9] a) R. Sugitani, A. A. Stuchebrukhov, *Biochim. Biophys. Acta Bioenerg.* **2009**, *1787*, 1140–1150; b) A. Tuukkanen, V. R. I. Kaila, L. Laakkonen, G. Hummer, M. Wikström, *Biochim. Biophys. Acta Bioenerg.* **2007**, *1767*, 1102–1106.  
[10] P. E. M. Siegbahn, F. Him, *Wiley Interdiscip. Rev.: Comput. Mol. Sci.* **2011**, *1*, 323–336.  
[11] a) M. Wikström, M. I. Verkhovsky, *Biochim. Biophys. Acta Bioenerg.* **2007**, *1767*, 1200–1214; b) V. R. I. Kaila, M. I. Verkhovsky, G. Hummer, M. Wikström, *Biochim. Biophys. Acta Bioenerg.* **2009**, *1787*, 1205–1214; c) P. E. M. Siegbahn, M. R. A. Blomberg, *Biochim. Biophys. Acta Bioenerg.* **2007**, *1767*, 1143–1156; d) P. E. M. Siegbahn, M. R. A. Blomberg, *J. Phys. Chem. A* **2008**, *112*, 12772–12780.  
[12] T. S. Zwier, *Science* **2004**, *304*, 1119–1120.  
[13] M. R. A. Blomberg, P. E. M. Siegbahn, *Biochim. Biophys. Acta Bioenerg.* **2012**, *1817*, 495–505.  
[14] J. M. Headrick, et al., *Science* **2005**, *308*, 1765–1769.  
[15] a) P. Goyal, S. Yang, Q. Cui, *Chem. Sci.* **2015**, *6*, 826–841; b) P. Goyal, J. Lu, S. Yang, M. R. Gunner, Q. Cui, *Proc. Natl. Acad. Sci. USA* **2013**, *110*, 18886–18891.  
[16] D. Riccardi, et al., *J. Phys. Chem. B* **2006**, *110*, 6458–6469.  
[17] a) Z. Cao, Y. Peng, T. Yan, S. Li, A. Li, G. A. Voth, *J. Am. Chem. Soc.* **2010**, *132*, 11395–11397; b) V. R. I. Kaila, G. Hummer, *Phys. Chem. Chem. Phys.* **2011**, *13*, 13207–13215.

- [18] a) M. Karpefors, P. Ädelroth, P. Brzezinski, *Biochemistry* **2000**, 39, 5045–5050; b) M. Karpefors, P. Ädelroth, P. Brzezinski, *Biochemistry* **2000**, 39, 14664–14669.
- [19] M. Wikström, C. Ribacka, M. Molin, L. Laakkonen, M. Verkhovsky, A. Puustinen, *Proc. Natl. Acad. Sci. USA* **2005**, 102, 10478–10481.
- [20] P. Goyal, N. Ghosh, P. Phatak, M. Clemens, M. Gaus, M. Elstner, Q. Cui, *J. Am. Chem. Soc.* **2011**, 133, 14981–14997.
- [21] V. R. I. Kaila, M. Wikström, G. Hummer, *Proc. Natl. Acad. Sci. USA* **2014**, 111, 6988–6993.
- [22] J. C. Phillips, et al., *J. Comput. Chem.* **2005**, 26, 1781–1802.
- [23] A. D. MacKerell, et al., *J. Phys. Chem. B* **1998**, 102, 3586–3616.
- [24] M. P. Johansson, V. R. I. Kaila, L. Laakkonen, *J. Comput. Chem.* **2008**, 29, 753–767.
- [25] H. L. Woodcock III, M. Hodoscek, A. T. Gilbert, P. M. Gill, H. F. Schaefer III, B. R. Brooks, *J. Comput. Chem.* **2007**, 28, 1485–1502.
- [26] a) A. D. Becke, *J. Chem. Phys.* **1993**, 98, 5648–5652; b) C. T. Lee, W. T. Yang, R. G. Parr, *Phys. Rev. B* **1988**, 37, 785–789; c) A. Schäfer, H. Horn, R. Ahlrichs, *J. Chem. Phys.* **1992**, 97, 2571–2577; d) S. Grimme, J. Antony, S. Ehrlich, H. Krieg, *J. Chem. Phys.* **2010**, 132, 1154104.
- [27] F. Weigend, R. Ahlrichs, *Phys. Chem. Chem. Phys.* **2005**, 7, 3297–3305.
- [28] A. Klamt, G. Schüürmann, *J. Chem. Soc. Perkin Trans. 2* **1993**, 799–805.
- [29] R. Ahlrichs, M. Bär, M. Häser, H. Horn, C. Kölmel, *Chem. Phys. Lett.* **1989**, 162, 165–169.
- [30] W. Humphrey, A. Dalke, K. Schulten, *J. Mol. Graphics* **1996**, 14, 33–38.

Received: April 13, 2016

Revised: June 7, 2016

Published online: August 19, 2016